

A Magnetic Properties and Corrosion Resistance of Fe-Si Alloy Coating Prepared on Mild Steel

Yi WANG^{1*}, Qiongyu ZHOU^{2,3}, Qingdong ZHONG³

¹ Shansteel Research Institute of Iron & steel, Shandong Iron & Steel Group Company Limited, Jinan, Shandong, 250101, PR China

² Institute of Applied Physics, Jiangxi Academy of Sciences, Nanchang, Jiangxi Province 330029, PR China

³ Shanghai Key Laboratory of Modern Metallurgy and Material Processing, Shanghai University, Shanghai, 200072, PR China

crossref <http://dx.doi.org/10.5755/j01.ms.20.4.6446>

Received 13 February 2014; accepted 11 November 2014

The present work deals with preparation of Fe₃Si coatings on mild steel and evaluation of its magnetic property and anti-corrosion behavior. Magnetic property of coatings was measured using a vibrating sample magnetometer. The results show that the saturation magnetization reached to the maximum value (214.1 emu·g⁻¹) and the coercivity fell to the lowest (23.11 Oe) at 1000 °C. Anti-corrosion of the coatings was studied using polarization in 3.5 % NaCl solution. It was found that the corrosion current density (*i*_{corr}) decreased with increasing of heat treatment temperature ranging from 700 °C to 1000 °C, indicating an improvement in corrosion resistance of Fe-Si alloy coating.

Keywords: nano-Si, mild steel, magnetic properties, corrosion resistance.

1. INTRODUCTION

There has been a lot of study on the progress of surface treatment process to improve electrical, thermal, mechanical properties, corrosion resistances and other specific performance meeting their needs [1–4]. Several attempts have been made to produce surface thin films or coatings by the techniques such as electro-deposition [5], physical vapor deposition (PVD) [5], chemical vapor deposition (CVD) [5, 6], thermal spraying [7, 8] and cold spraying [9, 10]. Thus, investigation in modern surface treatments is significant and meaningful for industrial applications.

It is well known that corrosion resistance of steel could be enhanced by adding appropriate amount of silicon [11, 12]. However, as previous literatures indicated, the strength and toughness would decrease by silicon alloying, which may cause their work ability damaged. For the purpose of improving the properties of the steel substrate meanwhile without damaging the mechanical properties of the bulk, a wide range of experimental treatment processes have been used, such as chemical vapor deposition, vacuum deposition and solid reaction with silicon powder [11, 12]. Pack-cementation is one of the most important industrial methods for preparation of low cost and good adhesion coating [13, 14]. Ueda et al. [15] applied the electrolytic plating of an iron substrate in the molten bath composed of LiCl-KCl-LiF-K₂SiF₆ at high temperature. K. Tatemoto et al. [16] adopted electroless plating simply by immersing Fe, Co, Ni, Mo, Nb or Cr plates into a molten salt (KCl-NaCl-NaF-Na₂SiF₆-Si) and then melted in Ar gas atmosphere to get different silicides on metal surfaces.

Fe_xSi has excellent soft magnetic property, high temperature oxidation resistance and corrosion resistance, all of which changes with Si contents. Specially, the alloy

which contains 6.5 wt.% Si is always considered as an ideal soft magnetic material, due to the fact that its saturation magnetostriction constant in the isotropic structure equals to almost zero [17]. There are also lots of research about effects of Si content, milling time or heat treatment on the formation and microstructure of Fe-Si alloy [18–21]. Abdellaoui et al. [18] concluded that the phase changes in the nanostructure Fe-Si alloy at different concentration of Si using mechanical alloying. Gaffet et al. Stevulova et al. [19] produced Fe-Si alloy in the nano-scale and found that microstructure changes with respect to the milling time. E. Gaffet [20] studied the phase transition of Fe-Si alloy as the function of the mechanical alloying and annealing. Zuo [21] investigated the effect of annealing on the ordering and grain growth of Fe-Si alloy.

With the above aspects as the backdrop, in this study, a simplified process was adopted for preparation of Fe-Si alloy coating on mild steel. Nano-hybrid particles (Fe₂O₃/Si) produced by high-energy ball mill and annealing under hydrogen atmosphere was applied to develop Fe₃Si coating. The powders proceed metallurgical reaction and combined into substrate. The corrosion resistance of coatings on mild steel varies as a function of heat treatment temperature and was evaluated by Tafel polarization.

2. EXPERIMENTAL DETAILS

2.1. Preparation of nano-hybrid particles and samples

In this coating procedure, Si was used as source and Fe₂O₃ as activator. Firstly, Si and Fe₂O₃ were laid inside a agate jar with a molar ratio of 1:2.5. Then, absolute ethanol, which served as the dispersing agent, was added in the agate jar, with the liquid solid ratio 80:15. After 12 hour ball-milling, hybrid powder was finally produced,

*Corresponding author. Tel.: +86-13706381117; fax: +86-053167607052. E-mail address: kasuo.9@163.com (Y. Wang)

with the average size of about 45 nm and the composition of Fe_2O_3 -6.55wt.% Si.

Mild steel ($10 \times 10 \times 2$ mm) was used as substrate, which was mechanically polished using 240, 400, 1200 grit papers to mirror face in sequence. Then the samples were rinsed in acetone, and water for 3 min respectively by an ultrasonic cleaner. Then Fe_3Si coatings were prepared on the surfaces of substrates by spraying nano-hybrid particles. The coatings' thickness was controlled at 40 μm and then dried at room temperature. A thermo chemical treatment was carried out at temperatures of 700 °C, 800 °C, 900 °C and 1000 °C for 4 h separately under hydrogen atmosphere with a heating rate of 15 °C /min.

2.2. Characterization of coating

After the thermo chemical treatments, the surface morphology and microstructure of coating were investigated by scanning electron microscopy (SEM) using a SU1510 microscope. The composition of the coating was investigated by X-ray diffraction (XRD) analysis with a diffractometer D/max-2550 V using radiation of $\text{Cu K}\alpha$. As for the test of magnetic property, the coatings were made on the surface of mild steel ($10 \times 10 \times 0.04$ mm), which is different from that of testing in SEM and XRD. The magnetic property of coatings was measured using a vibrating sample magnetometer (lakes hore7407, America) at room temperature.

The corrosion behavior of the coatings was studied using polarization techniques (Tafel) with an electrochemistry station (CHI660C). Tafel experiments for the substrate and the coatings were carried out in 3.5 wt.% NaCl solution at a potential sweep rate of 1 mV/s. A saturated calomel electrode (SCE) as reference- electrode and a platinum wire as counter-electrode were used in the tests. The surface area of the test coupons (as the working electrode) exposed to the electrolyte was 1 cm^2 .

3. RESULTS AND DISCUSSION

3.1. Microstructure

The surface morphology of coating at 700 °C is shown in Fig. 1, a. As shown in this figure, the coating is relatively homogenous, and almost no cracks can be found. However, large and loose particles, which cannot combine with mild steel, appears in the surface of the coating. The morphology of the coatings differed with increasing of thermal treatment temperature, (see Fig. 1, c and d). This phenomenon may be caused by the fusion of the surface particles and the diffusion of new metal atoms, which were generated by hydrogen reduction from oxides particles. Higher temperature promotes the fusing and the diffusion progress of the coating, thus improves the bond between the coating and the substrate. When heating temperature reaches 1000 °C, a compact coating without porous forms under the entire surface.

3.2. Cross-section morphologies analyses

As can be seen in Fig. 2, three distinct zones are identified on cross-sections: (i) a surface layer; (ii) a transition zone; (iii) the steel matrix. A compact layer is formed on all the four surfaces under different temperature. Except for the sample with heat treatment temperature of

700 °C, composite coatings of other samples combine well with the mild steel substrate. There are no obvious cracks or peelings are observed, which shows a good metallurgy bonding between composite coatings and the mild steel substrate. The thickness of surface layer and transition zone are affected by the heat treatment temperature. As the temperature increases, the thickness of surface layer decreases while transition zone's thickness increases, yet the added thickness of surface layer and transition zone increases under higher temperature and reached to 40 μm in the heat treatment temperature of 1000 °C.

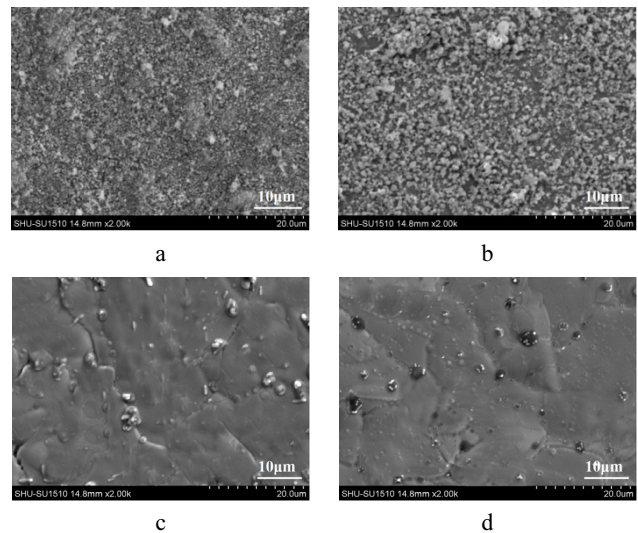


Fig. 1. Scanning electron micrographs of Fe-Si coatings: a – 700 °C; b – 800 °C; c – 900 °C; d – 1000 °C

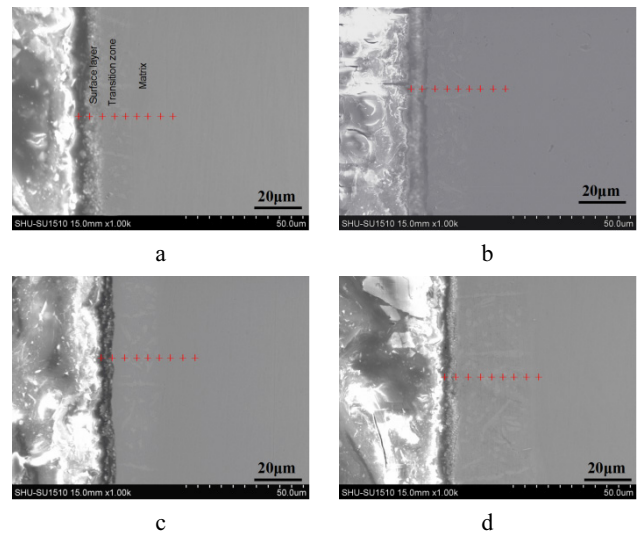


Fig. 2. Cross-section morphology of Fe-Si alloy coatings: a – 700 °C; b – 800 °C; c – 900 °C; d – 1000 °C

In order to determine the distribution of the element in the surface layer depth, we chose the surface of the samples as the zero starting point and picked another 8 points (the cross points shown in Fig. 2) every point is 5 μm away from one another, the farther the point is, the more distance they are away from the surface. It is obviously observed from Fig. 3 that the content of Si varies with heat treatment temperature. The content of Si decreases as the increasing of temperature on the outer

surface. Then, it shows a decrease as the distance gets deeper from the surface under the condition of all four temperatures. Finally, it reaches almost to the same content until the distance of 40 μm from the surface. The gap of Si contents from the surface to 40 μm inside decreases gradually with the increase of temperature. The Si content in surface layers and transition layers are slightly different, which is one of the reasons for the diversity of the cross sections' microstructure in the surface layer and transition layer. In addition, Si content in transition zone has no great difference as shown in the element analysis of the cross sections. Therefore, the composition is very consistent, which ensures the stability of the alloy layer performance.

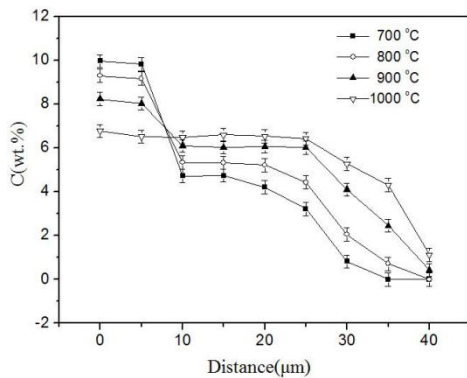


Fig. 3. Content of Si of Fe-Si alloy coatings

3.3. XRD analysis

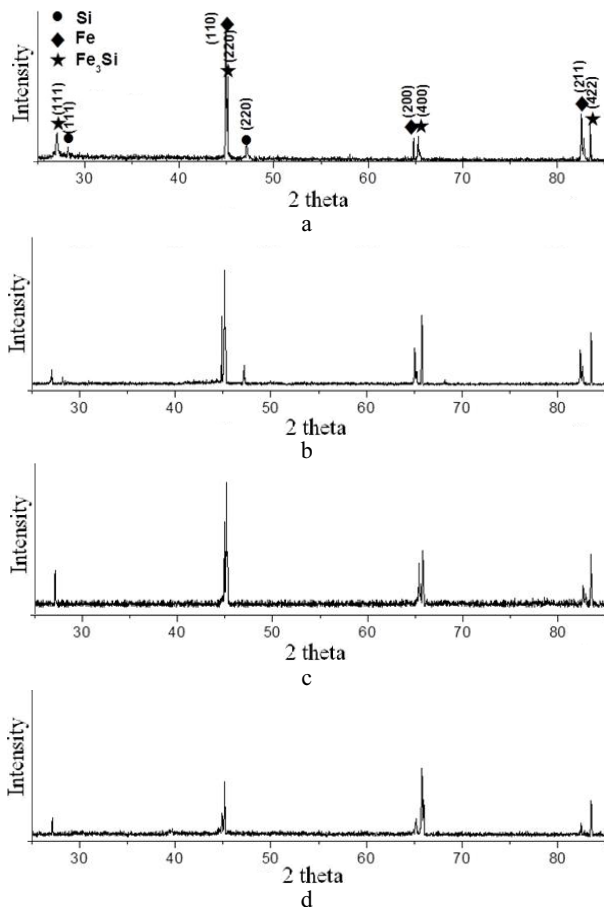


Fig. 4. XRD of Fe-Si alloy coatings: a – 700 °C; b – 800 °C; c – 900 °C; d – 1000 °C

After the coating preparation on the surface of mild steel which was used as substrate, the samples were heat-treated in a temperature range from 700 °C to 1000 °C. The XRD patterns of these samples are shown in Fig. 4. As shown in the figure, there are three diffraction peaks in 2θ values of 244.66°, 65.01° and 82.41° correspond to the iron(110), (200) and (211) crystal planes respectively. Diffraction peaks shown in 2θ values of 28.26°, 47.15° represent (111) and (220) crystal planes. Diffraction peaks in 2θ values of 27.20°, 45.19°, 65.79° and 83.50° correspond to Fe_3Si (111), (220), (400) and (422) [22] crystal planes respectively. Under lower temperature of 700 °C and 800 °C, Si and reducing Fe does not react completely with mild steel, thus resulting in elemental Fe, Si and Fe_3Si remaining on surface. Yet under higher temperature of 900 °C and 1000 °C, there are no diffraction peaks of Si found in XRD patterns, illustrating alloy layer on the surface of mild steel consists of only two phases of Fe-based solid solution and Fe_3Si . This is probably caused by the increase of atomic activity and diffusion ability resulting from the increasing of temperature. Diffraction peak intensity of Fe decreases relative to Fe_3Si as the temperature increases and the diffraction peaks of Fe is hardly observed by 1000 °C, showing the surface alloy layer consists of almost only Fe_3Si .

3.4. Magnetic property analysis

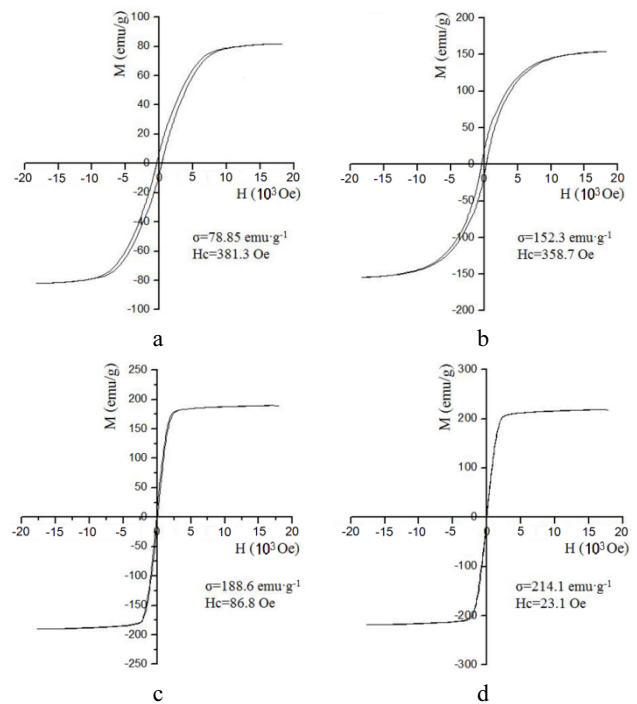


Fig. 5. Hysteresis loop of Fe-Si coatings: a – 700 °C; b – 800 °C; c – 900 °C; d – 1000 °C

By the hysteresis, when the heat preservation temperature is higher than 900 °C, the sample has higher specific saturation magnetization, lower coercivity and lesser area surrounded by the magnetic hysteresis loops. In another word, the hysteresis loss of alloy layers reduces with the increasing of temperature, which makes the alloy sample in 1000 °C owns the best soft magnetic property. It needed much bigger magnetic field strength when the magnetic induction intensity reaches the maximum value under

900 °C and 1000 °C than that under 700 °C and 800 °C, showing the samples in higher temperatures own lower magnetic sensitivity and relatively larger coercive force (H_c). When the temperature arrives at 1000 °C, the Si content of alloy layer is 6.5 wt.%, the sample reaches the maximum value of specific saturation magnetization and the minimum value of the coercive force. This is consistent with the common Fe-Si materials with single crystal and polycrystalline.

3.5. Evaluation of corrosion behavior

The corrosion resistance of coatings can be researched by potentiodynamic polarization tests. Cl^- is a kind of aggressive ion in electrolyte solution, which could penetrate through cracks and reach to mild steel. Therefore, substrate is oxy-genated and ferrous ions are formed. Ferrous ions diffuse to surface and internal of the coating. Then, the reaction of OH^- ions and ferrous ions in electrolyte solution generated ferrous hydroxide, and ferric hydroxide with further oxidation [10]. The processes are as described below:

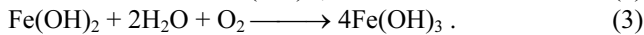
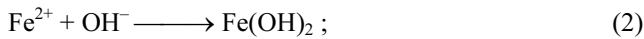
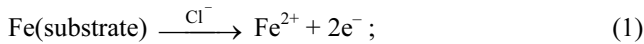


Fig. 6 shows the potentiodynamic polarization curves of mild steel and Fe-Si coatings. The data for corrosion potential (E_{corr}), corrosion current density (i_{corr}) and corrosion inhibiting efficiency ($E_{\text{resistance}}$) are tabulated in Table 1. $E_{\text{resistance}}$ is calculated by equation as follow:

$$E_{\text{resistance}} = \frac{i_{\text{corr}}^0 - i_{\text{corr}}}{i_{\text{corr}}^0} \times 100\%, \quad (4)$$

where i_{corr}^0 is the corrosion current density of mild steel; i_{corr} is the corrosion current density of sample (a, b, c or d).

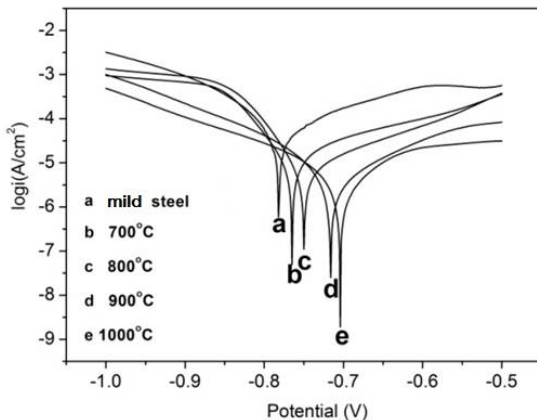


Fig. 6. Polarization curves of substrate and Fe-Si coatings: a – mild steel; b – 700 °C; c – 800 °C; d – 900 °C; e – 1000 °C

Table 1 Polarization tests parameters for substrate and Fe-Si coatings

Sample	$T, ^\circ\text{C}$	$E_{\text{corr}}, \text{V}$	$i_{\text{corr}}, \mu\text{A}\cdot\text{cm}^{-2}$	$E_{\text{resistance}}, \%$
Mild steel	–	–0.781	97.72	
a	700	–0.765	20.32	79.21
b	800	–0.751	7.52	92.30
c	900	–0.716	5.22	94.66
d	1000	–0.705	2.64	97.30

Anodic reaction in the potentiodynamic curve corresponds corrosion resistance of coatings. Meanwhile, cathodic potentiodynamic curve relates to the evolution of hydrogen. With the corrosion potential positive shift, corrosion current density is lower and corrosion resistance is stronger.

In comparison with mild steel, all Fe-Si coatings have much lesser corrosion current density and more positive corrosion potential. This phenomenon shows that the mild steel with coating enhanced significantly the ability of corrosion resistance for the Cl^- ions. In addition, the polarization curves will shift to the right side when increasing temperature, which means lesser corrosion current density and more positive potentials suggesting the endurance of corrosion resistance of the coatings at 1000 °C increased markedly. Among all samples, the mild steel treated at 1000 °C shows the most noble potential ($E_{\text{corr}} = -0.705 \text{ V}$), the minimum corrosion current density ($i_{\text{corr}} = 2.64 \mu\text{A}/\text{cm}^2$) and the largest corrosion inhibiting efficiency ($E_{\text{resistance}} = 97.30 \%$), which could be due to the relatively compact grain and consistent structure of coating.

4. CONCLUSIONS

This feasible study develops a useful type coatings (Fe_3Si) on the surfaces of mild steel. A compact structure was observed. X-ray diffraction studies confirmed that the coating prepared at 1000 °C was constituted of Fe_3Si phase without any other intermetallic phase. Depending on the process temperature, the saturation magnetization of coated samples ranged from $78.85 \text{ emu}\cdot\text{g}^{-1}$ to $214.1 \text{ emu}\cdot\text{g}^{-1}$ and the coercivity of coated samples ranged from 381.3 Oe to 23.11 Oe. The saturation magnetization reached to the maximum value and the coercivity falls to the lowest in 1000 °C. Polarization test results showed that the coatings provided proper corrosion protection for the mild steel substrate and it obtained the best corrosion resistance in 1000 °C.

Acknowledgments

This paper is financially supported by program for State Key Laboratory of Development and Application Technology of Automotive Steel (Bao. Steel) and New Century Excellent Talents in University NCET-07-0536.

REFERENCES

1. Makii, K., Yaguchi, H., Kaiso, M., Ibaraki, N., Miyamoto, Y., Oki, Y. Influence of Si on Nano Sub-structure of Cementite Lamellae in Pearlitic Steel Wires *Scripta Materialia* 11 1997: pp. 1753–1758.
2. Tsipas, D., Noguera, H., Rus, J. Corrosion Behaviour of Boronized Low Carbon Steel *Materials Chemistry and Physics* 18 (3) 1987: pp. 295–303.
3. Dong, M., Shen, B. L., Chao, Y., Xin, Z. Microstructure Analysis of Boronized Pure Nickel Using Boronizing Powders with SiC As Diluent *Vacuum* 83 2009: pp. 1481–1486.
4. Ozkan, O., Metin, U., Cuma, B., A. Hikmet, U. Hard Iron Boride (Fe_2B) on 99.97 wt% Pure Iron *Vacuum* 80 2006: pp. 1391–1396.

5. **Tjong, S. C., Chen, H.** Nanocrystalline Materials and Coatings *Materials Science and Engineering R* 45 2004: pp. 1–3.
<http://dx.doi.org/10.1016/j.mser.2004.07.001>
6. **Li, D. Y., Szpunar, J. A.** A Monte Carlo Simulation Approach to the Texture Formation during Electrodeposition. I – The Simulation Model *Electrochimica Acta* 42 1997: pp. 37–42.
[http://dx.doi.org/10.1016/0013-4686\(96\)00164-8](http://dx.doi.org/10.1016/0013-4686(96)00164-8)
7. **Choy, K. L.** Chemical Vapour Deposition of Coatings *Progress in Materials Science* 48 2003: pp.57–61.
8. **He, J., Schoenung, J. M.** Nanostructured Coatings *Materials Science and Engineering A* 336 2002: pp. 274–282.
[http://dx.doi.org/10.1016/S0921-5093\(01\)01986-4](http://dx.doi.org/10.1016/S0921-5093(01)01986-4)
9. **Papyrin, A.** Cold Spray Technology *Advanced Materials and Processes* 159 2001: pp. 49–54.
10. **Wang, H. T., Li, C. J., Yang, G. J., Li, C. X.** Cold Spraying of Fe/Al Powder Mixture: Coating Characteristics and Influence of Heat Treatment on The Phase Structure *Applied Surface Science* 255 2008: pp. 2538–2544.
11. **Byalobzheskii, A. V., Tsirlin, M. S., Krasilov, B. I.** High-Temperature Corrosion and Protection of Superrefractory Metals. Atomizdat, Moscow, 1977.
12. **Saldanha, B. J., Streicher, M. A.** Effect of Silicon on the Corrosion Resistance of Iron in Sulfuric Acid *Materials Performance* 25 1986: pp. 37–43.
13. **Bianco, R., Harper, M. A., Rapp, R. A.** Codepositing Elements by Halide-activated Pack Cementation *Journal of the Minerals Metals & Materials Society* 43 (11) 1991: pp. 68–73.
<http://dx.doi.org/10.1007/BF03222724>
14. **Li, Y., Soboyejo, W., Rapp, R. A.** Oxidation Behavior of Niobium Aluminide Intermetallics Protected by Aluminide and Silicide Diffusion Coatings *Metallurgical and Materials Transactions B* 30 (3) 1999: pp. 495–504.
15. **Ohzuku, T, Ueda, A, Yamamoto, N, et al.** Factor Affecting the Capacity Retention of Lithium-ion Cells *Journal of Power Sources* 54 (1) 1995: pp.99–102.
16. **Tatemoto, K., Ono, Y., Suzuki, R. O.** Silicide Coating on Refractory Metals in Molten Salt *Journal of Physics and Chemistry of Solids* 66 2005: pp. 526–534.
17. **Bozorth, R. M.** (Ed.). Ferromagnetism. D. Van Nostrand, New York, 1951: pp. 649–651.
18. **Abdellaoui, M., Djega-Mariadassou, C., Gaffet, E.** Structural Study of FeSi Nanostructured Materials *Journal of Alloys and Compounds* 259 1997: pp. 241–248.
[http://dx.doi.org/10.1016/S0925-8388\(97\)00102-3](http://dx.doi.org/10.1016/S0925-8388(97)00102-3)
19. **Stevulova, N., Buchal, A., Petrovic, P., Tkacova, K., Sepelak, V.** Structural Investigation of the High-energy Milled Fe–Si System *Journal of Magnetism and Magnetic Materials* 203 1999: pp. 190–196.
[http://dx.doi.org/10.1016/S0304-8853\(99\)00224-3](http://dx.doi.org/10.1016/S0304-8853(99)00224-3)
20. **Gaffet, E., Malhouroux, N., Abdellaoui, M.** Far from Equilibrium Phase Transition Induced by Solid-state Reaction in The FeSi System *Journal of Alloys and Compounds* 194 1993: pp. 339–346.
[http://dx.doi.org/10.1016/0925-8388\(93\)90020-N](http://dx.doi.org/10.1016/0925-8388(93)90020-N)
21. **Zuo, B., Sritharan, T.** Ordering and Grain Growth in Nanocrystalline Fe₇₅Si₂₅ Alloy *Acta Materialia* 53 2005: pp. 1233–1239.
<http://dx.doi.org/10.1016/j.actamat.2004.11.017>
22. **Cherigui, M., Fenineche, N. E., Ji, G., Grosdidier, T., Coddet, C.** Microstructure and Magnetic Properties of Fe-Si-based Coatings Produced by HVOF Thermal Spraying Process *Journal of Alloys and Compounds* 427 2007: pp. 281–287.
<http://dx.doi.org/10.1016/j.jallcom.2006.03.005>